FEM Analysis of Split Electrode IDTs Designed Lithium Tantalate-Polyaniline SAW Gas Sensor

Dhananjaya Panda and Koteswara Rao Peta(✉)

Department of Electronic Science, University of Delhi South Campus, Benito Juarez Road, New Delhi 110012, India
krao@south.du.ac.in

Abstract. The finite element method (FEM) underpinning COMSOL Multiphysics 6.0 has been used to model the sensing of various polar volatile organic compounds (VOCs) by the split electrode interdigital transducers (SEIDT) surface acoustic wave (SAW) sensor. On a $LiTaO_3$ base, split-electrode interdigital transducers were employed with a sensing layer of polyaniline (PANI). Acetone VOC gas was detected using a SAW sensor at RT with a concentration of 100 ppm. After the gas specimen interacted with the detecting polymer, a change in the density of the sensing surface was seen, and with it, a change in the Rayleigh wave's Eigen frequency. For a number of studies, we measured admittance, displacement, quality factor, and electric potential versus frequency in addition to plotting the deformed shape at the Eigen (resonance) frequency. The S-parameter and quality factor studies also demonstrate the benefits of using split electrode IDTs in SAW sensors for lowering reflection loss.

Keywords: VOCs · FEM · COMSOL · Split electrode IDT · Polyaniline (PANI)

1 Introduction

Gases in the atmosphere are essential for both living and nonliving organisms. Due to the growth in pollutant gases in the atmosphere, it is crucial for environmental and diagnostic reasons to detect dangerous gases at the micro level. Several gases may be detected by a gas sensor in our digitalized and technological age [1, 2]. The mass sensitivity, lesser environmental disturbance, lower power consumption, and mobility of the acoustic wave-based gas sensor make it very appealing.

Based on how the waves move, this acoustic wave sensor is divided into two parts: bulk acoustic wave (BAW) [3] and surface acoustic wave (SAW) sensor [4]. The SAW sensor device is made up of a substrate made of a piezoelectric material, an interdigital transducer (IDT) made of a conductive material, and a sensitive sensing layer that reacts to a specific gas. IDT is used to lay out the SAW device by putting the sensing layer on the pattern of the piezoelectric substrate. SAW based on a two-port Rayleigh resonator with a polymer-coated sensing layer has high sensitivity, higher stability, good response time, and low noise for gas detection [5, 6]. Due to its higher sensitivity and faster response time, SAW has been used for a wide range of applications, such as analysis of

A. K. Pandey et al. (Eds.): MAMM 2022, 126, pp. 250–265, 2023.
https://doi.org/10.1007/978-3-031-20353-4_20

gas and bio analyte in the lower levels of ppm, electronic nose in industrial installations, monitoring and protection of environmental issues, and medical applications [7–11]. The SAW sensor works because the response signal changes depending on how much the analyte weighs. When a specific analyte interacts with a surface acoustic wave (SAW), it gives off a specific frequency, which is picked up by the output circuitry.

Transducers, one of the three main parts of SAW sensors, have a big effect on how waves travel and how they interact with each other. Interdigitated transducers (IDTs) with specific shapes and sizes cause a certain wave to appear on the surface. The unique design of IDTs has solved some of the most important problems with SAW sensors, such as insertion loss, getting a high center frequency, etc. Different IDT parameters, like the width of the electrodes, the distance between the electrode fingers, the number of electrode fingers, and the size of the aperture, change the electrical impedance and frequency bandwidth, which affects how the wave spreads on the substrate. Compared to various IDTs structures, split electrodes have better control on insertion loss, eliminate reflections, self-resonance, and access to higher frequencies at the third harmonic [4, 12, 13]. The quality factor (Q Factor) is the parameter to measure the energy loss in the SAW device. The Q factor is the energy ratio between stored energy to the supplied energy. To get a high a stability of the SAW devices, the energy losses should be very less which is only possible by a high Q Factor. To achieve the high Q factor, a paired electrode has been developed in SAW device and named as split electrode interdigital transducers (SEIDT). The SEIDT configuration is also called meander line because of generation of third harmonic wave. These third harmonic wave have stronger response then the original wave.

Computer-aided design (CAD) using the finite element method (FEM) is a useful tool for developing action plans for research. COMSOL Multiphysics, a commercial finite element analysis product, provides a more robust modeling environment for developing SAW sensors [14, 15]. Zheng et al. [16] investigated sensing and how sensor layer spacing influenced gas detection. The SAW sensor was designed using layers of varying thicknesses on a $LiNbO_3$ substrate. The suggested SAW has a 100 nm, 200 nm, and 300 nm thick Si_3N_4 layer under a 100 nm to 1000 nm thick ZnO layer and a layered structure of ZnO, SiO_2, and $LiNbO_3$. The thickness of the sensing layer is directly proportional to the wave frequency and relies on the velocity of the surface waves, according to the study given here. Jakubik and colleagues [17] created a bilayer conductive material for SAW gas sensors. His study suggests that having many layers with distinct properties might increase sensitivity. Those researchers created various SAW structures for use in sensors. A lithium tantalate ($LiTaO_3$) piezoelectric substrate is topped with a polyaniline (PANI) sensing layer in this example ($C_{48}H_{38}N_8$).

2 Model Design

COMSOL is used for the design and modeling of SAW structures using a variety of physics. Lithium tantalate is used in this configuration as the piezoelectric substrate material for detecting gases. In order for surface acoustic waves to travel effectively, this $LiTaO_3$ material needs to have a high wave velocity. Since polyaniline (PANI) is very gas-sensitive, it is often utilized as a sensing layer [18–20]. In this paper, the device

dimensions and the 3D and 2D structures of SAW devices are shown in detail for a better understanding of the devices. In the 3D layout of the SAW sensor, a thin layer of PANI sensing materials (with dimensions of 1 μm in width, 0.6 μm in depth, and 0.05 μm in height) is drawn beneath a wider layer of substrate (with dimensions of 4 μm in width, 1 μm in depth, and 0.5 μm in height). Aluminum electrode splits on substrates with dimensions of 0.02 μm in width, 0.5 μm in depth, and 0.045 μm in height. Twelve sets of IDTs (24 electrodes) are drawn in this 3D SAW sensor design, with each pair of electrodes considered to be one IDT of the same dimension. Figure 1a depicts the 3D SAW sensor described above, which uses split electrodes (double electrodes). The grating structure of the planned SEIDT has an electrode interval of λ/8, electrode width of λ/8, and center-to-center distance of λ/4 (Fig. 1b). Only with the correct electrode dimensions and spacing will the meander line be formed (λ/8 + λ/8 + λ/8 = 3λ/8), which is what generates the third harmonic wave and what ultimately causes the reflection loss to be lowered Reflection loss in a SAW device is shown as a function of the scattering parameter (S parameter), more specifically the input reflection coefficient (S_{11}).

Figure 1b depicts the IDTs with the correct dimensions and spacing. Six sets of electrodes pair serve as input IDTs, while the remaining six serves as output IDTs. Due to the symmetry of each IDT, only two sets of IDTs will function as a complete sensor in the 2D design of the SAW gas sensor. Figure 2 depicts the schematic geometry of the 2D version of the SAW gas sensor with sensing layer, with the correct leveling and indication.

3 Simulation Methodology

The COMSOL Multiphysics program, version 6.0, was utilized in the course of this study to carry out the design of the SAW gas sensor. On the basis of partial differential equations (PDEs), this piece of software has enabled every stage of the design and development process, including modeling, physics specifications, and graph plotting. Through the use of a variety of tools and the application of physical principles, this software is used to create both 3D and 2D SAW sensor designs. This section contains an explanation of a variety of design factors, mathematical formulae, and physics calculations that were done.

Before beginning to create the design, the initial step of SAW design is to integrate physics to the simulation. As the material of interest is piezoelectric and the analysis is based on frequency response, the piezoelectricity domain should be included. In structural mechanics physics, the piezoelectricity domain is accessible in electromagnetic-structure interaction. In this SAW gas sensor analysis, both piezoelectric behavior and gas detection occurred concurrently. In the input port of the SAW IDTs, the direct piezoelectric effect will generate a wave on the surface of the substrate, which will travel to the end (output) port of the SAW IDTs, where the inverse piezoelectric behavior will convert the wave into electric with a change in frequency, causing the signal processor to display an indication. During the study of gas sensing, it is essential to evaluate many characteristics for gas analysis, such as displacement curve, potential increase, and Eigen frequencies. The periodic unit cell of the 2D geometry SAW device is shown in Fig. 2. The 2D geometry is shown to illustrate the COMSOL design parameters. The SAW

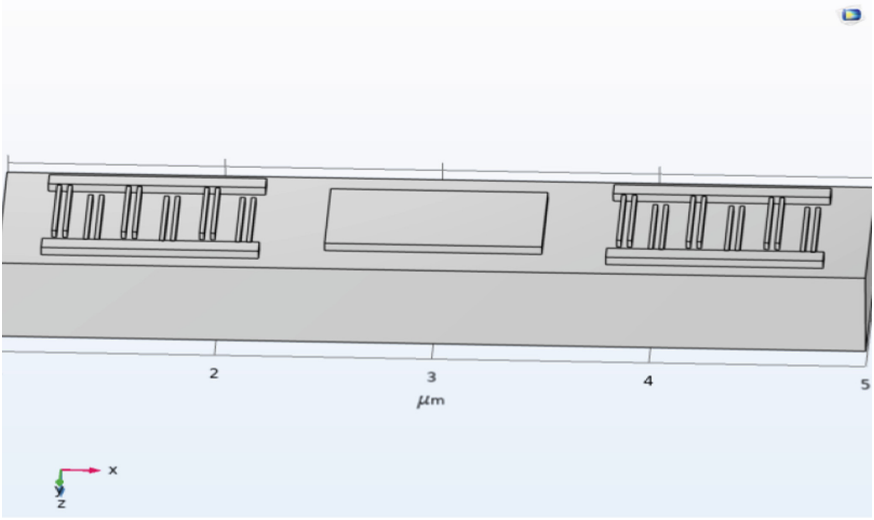

(a)

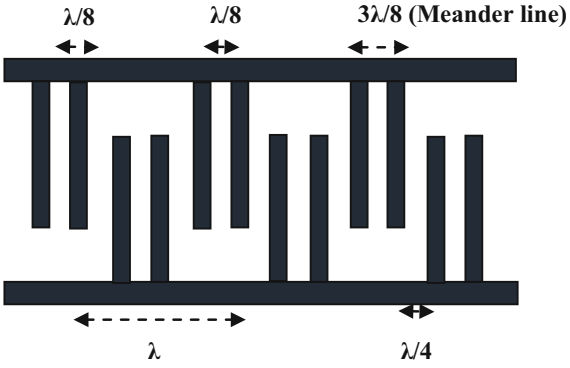

(b)

Fig. 1. Schematic of (a) SAW gas sensor design & (b) split electrodes with dimensions.

device's parameters are shown in Table 1. These parameters are the first input to the program before providing the SAW device's dimensions and meshing. The determined eigenfrequency represents the device's resonant frequency.

In order to comprehend the variation in frequency shift caused by both acetone gas and mass loading, it is essential to have a fundamental understanding of the mathematics behind the phenomenon. Some of the key points include wave propagation, gas concentration, the effect caused by mass loading, frequency shift, gas density, and gas ppm level. The equation that describes how waves move over the surface of the substrate is called the propagation equation (1).

$$T = C_E \times S - e^T \times E \tag{1}$$

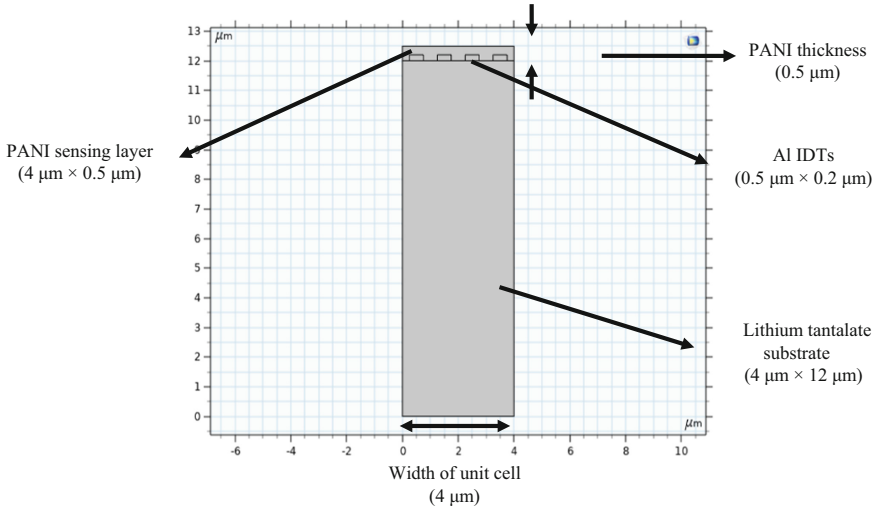

Fig. 2. Schematic diagram of 2D SAW gas sensor design.

Table 1. SAW Model parameters.

Variable	Values	Description
T	25 °C	Atmosphere temperature
P	1 atm	Atmosphere pressure
C_0	100	Acetone concentration (ppm)
C acetone air	$1e^{-6}$*C_0*P/(R-Constant*T)	Acetone concentration in air
M Acetone	58.08 g/mol	M Molar mass of gas
Rho-PANI	1.329 g/cm3	Density of PANI
E-PANI	4.42 GPa	Young's modulus of PANI
nu-PANI	0.3	Poisson's ratio of PANI
vR	3488 m/s	Rayleigh wave velocity
t-PANI	0.5 μm	PANI thickness
Width	4 μm	Width of unit cell
f_0	vR/width	Estimated SAW frequency

where, T = The stress matrix, C_E = Elasticity matrix, e^T = Piezoelectric matrix and E = electric field intensity.

Mass loading impact on a SAW sensor causes a change in the sensor's center frequency, among other effects. The molar mass of the gas has a significant impact on the resonance frequency shift of the piezoelectric materials. Ace-tone has a mol mass of 58.68 g per mole. To begin designing the sensor, it is necessary to consider the following

parameters.

$$C = \left(Co \times 10^{-6} \times P\right) \times RT^{-1} \tag{2}$$

$$\rho_{gas} \text{ in PANI} = K \times M \times C \tag{3}$$

$$\rho_{total} = \rho_{PANI} + \rho_{gas/PANI} \tag{4}$$

where, P = Atmospheric pressure (760 mmHg), R = gas constant (8.31 $Jmol^{-1}K^{-1}$), T = Temperature of air (298.15 K), K = The air/PANI partition coefficient for gas, Co = Gas concentration (in ppm), M = Molar mass of gases, and C = Concentration of gas in air. ρPANI = Density of PANI film (In absence of acetone to substrate) and ρ_{gas}/PANI = Density of PANI film (in presence of acetone gas).

The density of acetone gas in the presence of the sensing layer may be found by using Eq. (3) [21] (PANI). The density of the sensing layer shifts as a result of changes brought about by the adsorption of gases on the substrate. Equation may be used to determine the resonance frequency equation (5).

$$\nu = \lambda \times f_o \tag{5}$$

where, λ = Wavelength of wave, f_o = Resonance frequency, and ν = 3.488 ms^{-1} is the wave velocity in the piezoelectric substrate ($LiTaO_3$).

Various forms of wave propagation were discovered during the study of gas sensing. The wave is generated in a 2D SAW with a split electrode arrangement, where the first two electrodes are fed at zero potential and the second two are linked to a floating potential. Waves with a central frequency are caused by this alternating potential between two sets of electrodes. To ensure accurate alignment in the SAW sensor setup, mesh generation is performed once the structure has been specified with input parameters and physics. The 2D geometry of the SAW sensor is shown below in Fig. 3 with a fine mesh. After the mesh mapping was complete, the SAW sensor ran a series of computations to analyze its electrical and mechanical components.

4 Results and Discussions

Within a SAW sensor, the gas that is being monitored by the acoustic wave will travel along the piezoelectric material. The change in frequency of the resonance that occurs in response to the mass load of the sensing gas. During the course of this investigation, a shift in frequency caused by gas was discovered close to the Rayleigh wave frequency (the central frequency), as well as six eigen frequency discoveries close to the central frequency. Changing the gas, its concentration level, and other input parameters associated with the study are examples of changes that can occur during a parametric study. However, a researcher can easily change the parameters by studying the change in frequency in accordance with their particular area of interest, which is sensing gas. In the work being done on this research project, acetone gas is considered a primary detecting gas in comparison to other gases. This gas sensing performance is carried out at room temperature.

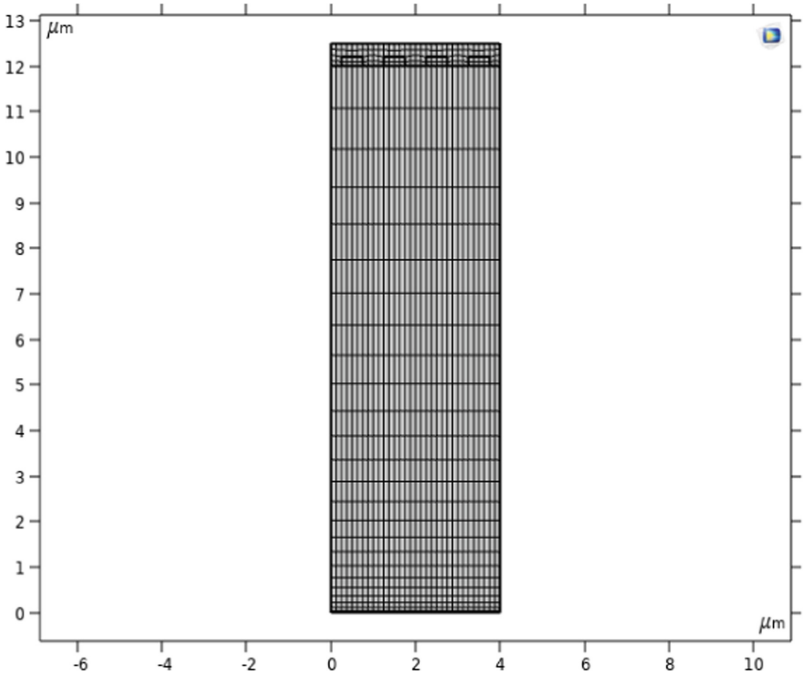

Fig. 3. Meshing to the 2D SAW geometry.

(a) Resonance and antiresonance plot.

The resonance and antiresonance frequencies of the SAW device are shown in the below Fig. 4. The real resonance frequency of the device was discovered to be 872 MHz while it was not exposed to gas; however, the resonance frequency that was computed after the device was exposed to gas was 825.67 MHz. It has been proved beyond a reasonable doubt that the acetone gas is responsible for the shift in resonance frequency, and the amount of the shift in resonance frequency of this SAW sensor is 46.33 MHz. Calculations of the SAW sensor's resonance frequency are shown in Table 2 with and without the presence of gas exposure.

Table 2. Frequency shift for acetone gas.

Gas	Resonance frequency (absence of acetone gas) (MHz)	Resonance frequency (presence of acetone gas) (MHz)	Frequency shift (MHz)
Acetone	872	825.67	46.33

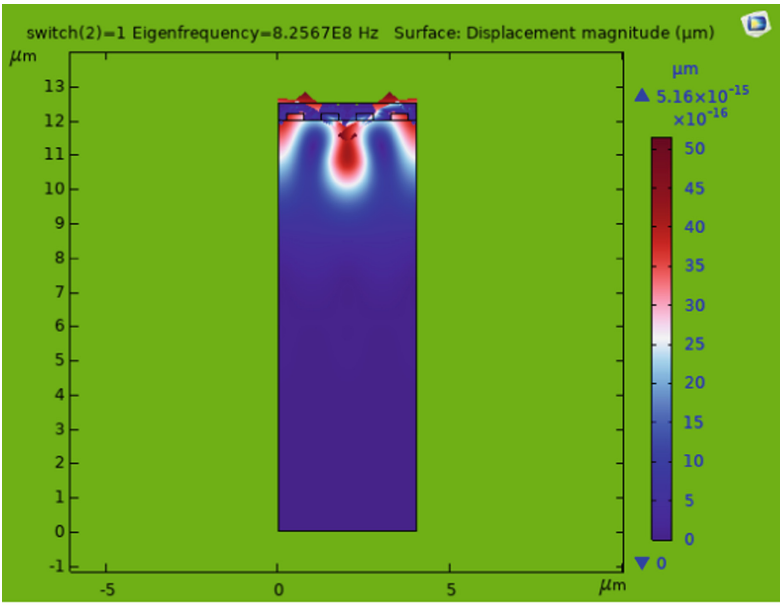

(a)

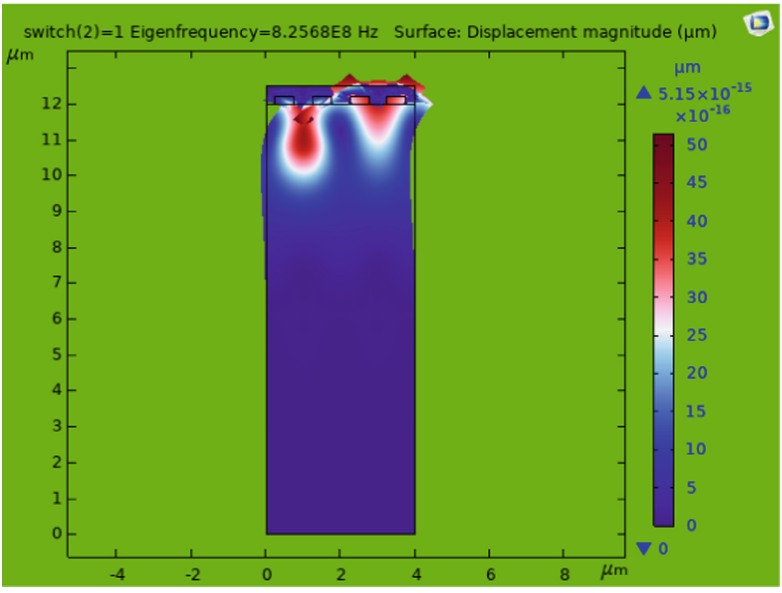

(b)

Fig. 4. Image of total displacement of (a) resonant frequency at 825.67 MHz and (b) anti-resonant frequency at 825.68 MHz of SAW senor.

(b) Electric potential distribution plot.

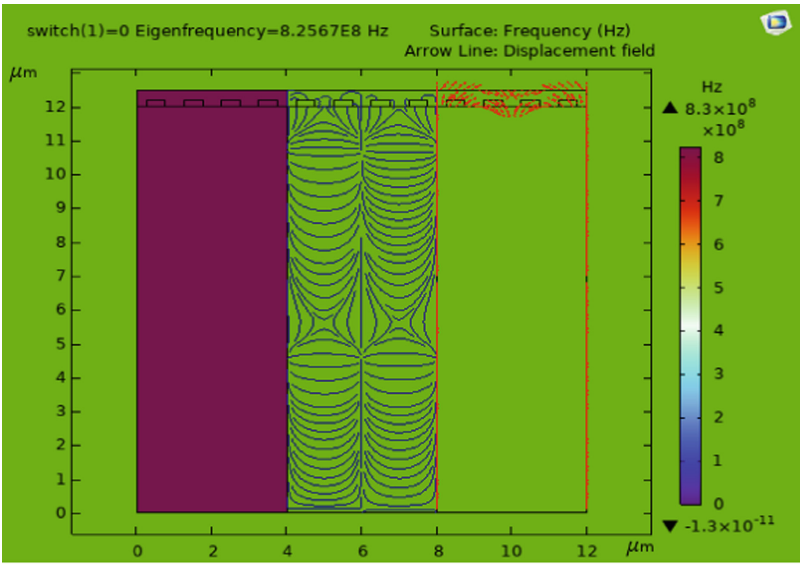

(a)

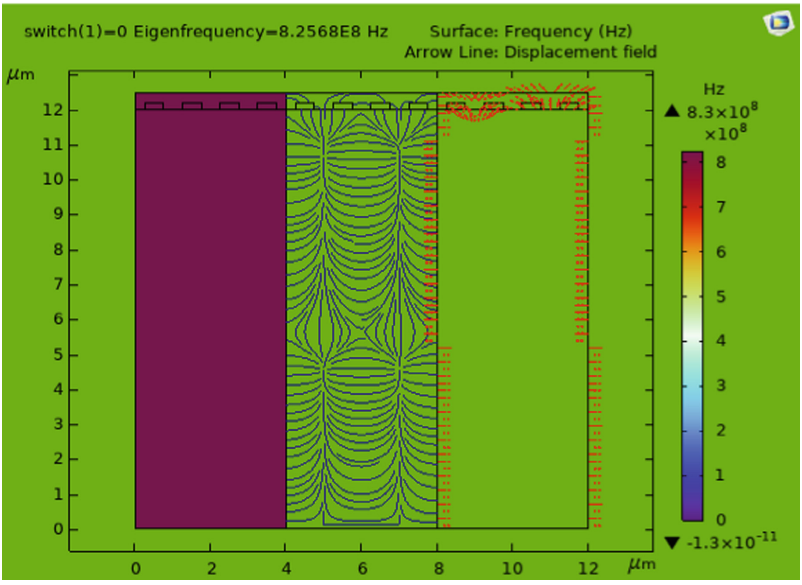

(b)

Fig. 5. Image of electric potential of (a) resonant frequency at 825.67 MHz and (b) anti-resonant frequency at 825.68 MHz of SAW sensor.

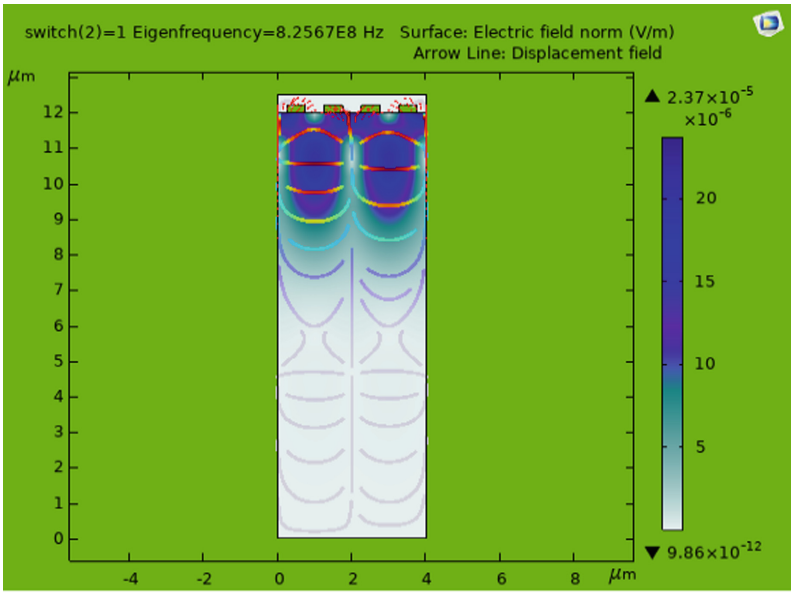

(a)

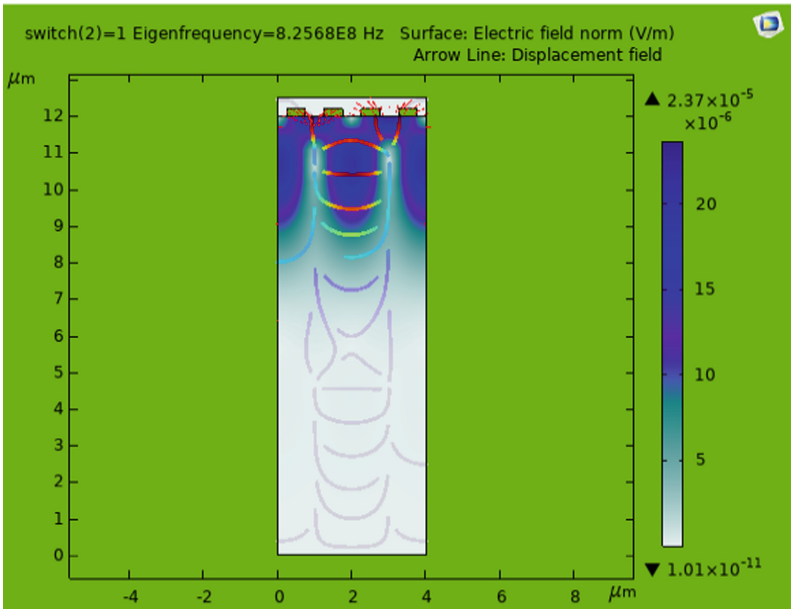

(b)

Fig. 6. Image of electric field normal at (a) resonant frequency at 825.67 MHz and (b) anti-resonant frequency at 825.68 MHz of SAW sensor.

(c) Electric field normal plot.

Figure 4 explains how far waves move on the surface at the frequency of resonance and the frequency of anti-resonance. The total displacement shows how mechanical waves travel through the substrate. Figure 5 shows the electric potential of a wave that is moving. Figure 5 shows how positive potential lines are spread out for resonant and anti-resonant frequencies. In the resonance frequency case, the electric potential is spread out properly. In the anti-resonance frequency case, the electric potential is also spread out along the side walls of the substrate. In this split electrode structure, two fingers are first connected to two floating potentials, and the other two are connected to the ground. Figure 6 shows the electric field normal of the propagating wave, which explains the tangential components of the surface for the flow of surface current.

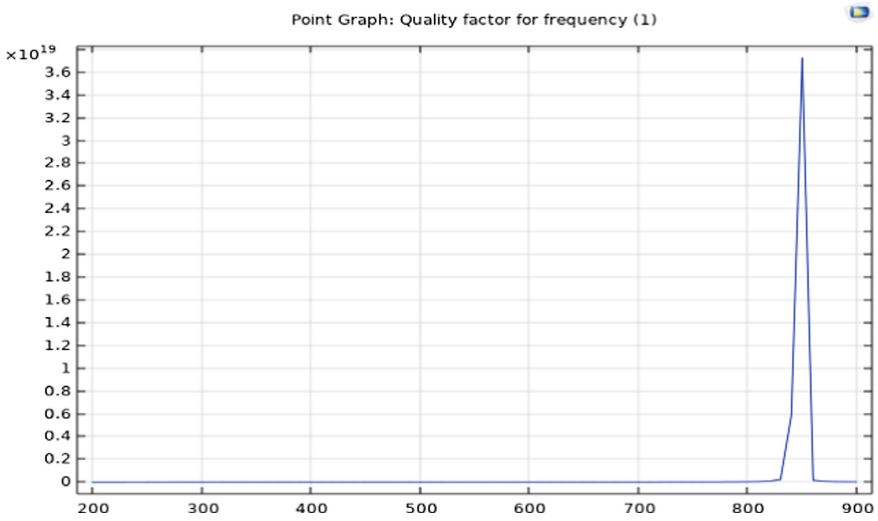

Fig. 7. Q Factor vs frequency curve for designed SAW device.

(d) Quality factor (Q factor) plot.

The Q Factor (Quality Factor) at resonant frequencies is seen in Fig. 7. As can be seen, the achieved Q factor for this surface wave resonant frequency is greater than 3.6×10^{19}. As can be seen in Fig. 7, a high Q factor results in less input-side reflection and thus reduced energy loss. Electric energy of the wave at the resonance frequency is seen in Fig. 8. Clearly seen in Fig. 8, the SAW wave has undergone a transformation in electric energy at its resonance frequency.

(e) Electric energy plot at resonance frequency.

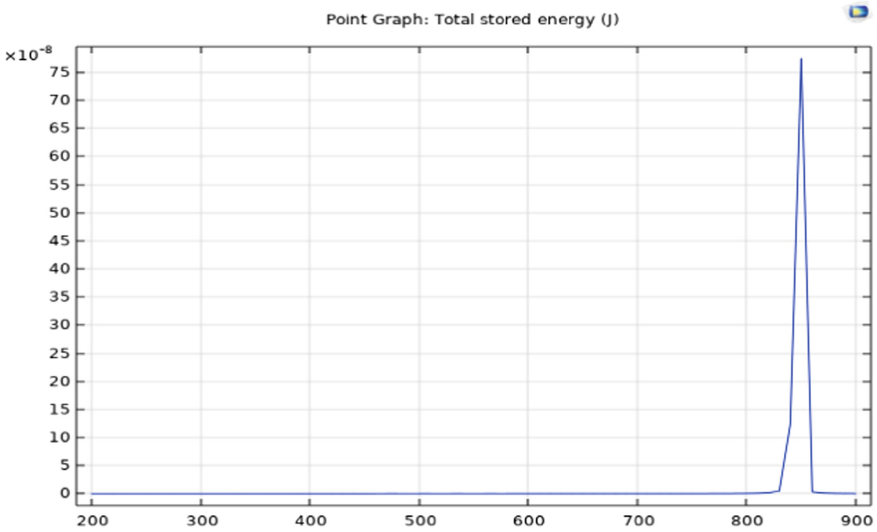

Fig. 8. Total electric energy curve at resonant frequency.

(f) Scattering parameter (S_{11} parameter) plot.

S-parameter analysis provides insight into the reflection coefficients, stability, power gains, etc. of any high-frequency circuit. To avoid problems with source-end reflection, a split-electrode IDTs configuration is provided here. Input reflection coefficient, expressed as a number between −11 dB and 0, is explained by the S_{11} parameter. At the resonance frequency, as shown in Fig. 9, the highest S-parameter is more than −11 dB, indicating that there is no reflection loss at the source. This SEIDT-based SAW gives improved control over the amount of reflection loss in comparison to bi-directional IDT-based SAW sensors [22]. The S_{11} value of the proposed SEIDT SAW sensor is lower than the S_{11} value (−8.856 dB) of the bi-directional IDT (two port) SAW sensor [22], which means that the bi-directional IDT (two port) SAW sensor has a higher S_{11} value. As a result of this study, it has been shown that SAW with SEIDT has a reduced S_{11}, which is essential for achieving a low reflection loss. In the experimental research work performed by Nguyen et al., the designed IDTs were double-split fingers with a finger length of 3.6 mm, a total IDT width of 3.2 mm, and space between IDTs of 4 μm [23] on the $LiTaO_3$ substrate. In millimeters, the finger length and total IDT width were measured, yielding an S_{11} value of −60 dB. The foremost reason of S_{11} is −60 dB because IDT was placed in a 4-(2-hydroxyethyl)-1-piperazineethanesulfonic acid (HEPES) buffer solution. When compared to the SEIDT SAW sensor, the high reflection coefficient is caused by the way the SAW wave moves through the HEPES buffer solution. In Table 3, we can see the differences between the proposed SEIDT SAW designs and the different IDT-based SAW structures.

Table 3. Comparison of different parameters of various SAW sensors.

Parameters	[22]	[23]	Present paper
Substrate	GaN/Si	36° Y-cut $LiTaO_3$	$LiTaO_3$
IDT structure	Bi-directional electrodes	Double split IDT	Split electrode IDT
S_{11} parameter (dB)	−8.856	−60	−11
Analyte	NA	NA	Acetone
Medium	Air	4-(2-hydroxyethyl)-1-piperazineethanesulfonic acid (Buffer solution)	Air
Resonance frequency (RF)	5.5 GHz	130 MHz	872 MHz 825.67 MHz (exposing gas)
Dimensions	(a) IDT range in "nm" (b) IDT Length = 100 μm, width = 200 nm	(a) IDT range in "mm" (b) IDT Length = 3.6 mm, width = 3.2 mm	(a) IDT range in "μm" (b) IDT Length = 0.5 μm, width = 0.2 μm
Remark	(a) More reflection at the output end because of simple IDTs (b) Due to the "nano meter" range IDT size, SAW device has high RF	(a) Very minimal reflection loss occurs as a result of the wave prorogate in the buffer medium (b) IDTs dimension are in "milli meter" range lead to very low RF	(a) The SEIDT topology significantly reduces reflection loss in comparison to [22] (b) Achieved higher reflection loss compared to [23] because of the air medium and higher RF

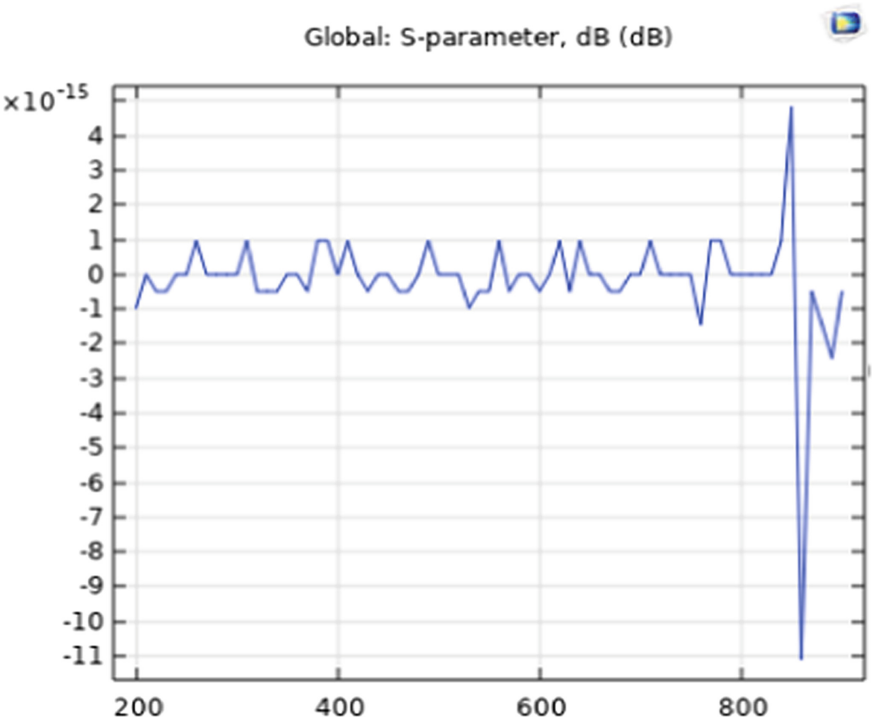

Fig. 9. S-parameter in dB at resonant frequency of SAW sensor.

5 Conclusions

In this study, COMSOL Multiphysics simulation software was used to plan the SAW gas sensor. Due to the symmetry of IDTs, the design of the SAW sensor is shown in both 3D and 2D, whereas all computations are done in the 2D version of the SAW sensor. Frequency-dependent analyses of SAW sensors, including electric potential distribution, total displacement, electric field norm, electric energy curve, and s-parameter, have been shown. The primary goal of this study is to develop a split electrode that may be used to lessen the reflection loss at the origin. The Q factors at resonance frequency, predicted to be 3.6×10^{19} for this research, are crucial to reducing reflection loss. Reduced energy dissipation and reflection result from a high Q factor. To further demonstrate the reduced energy loss or reflection loss, another research, such as S parameters, has been calculated. There is a sweet spot for the S_{11} parameter at -13 dB. According to the findings, the S_{11} parameter has a value of -11 dB, which is better than the minimum value of -13 dB required to achieve the lowest reflection loss on the transmitted signal at the input. The SAW sensor's resonant and anti-resonant frequencies to the acetone gas were 825.67 MHz and 825.68 MHz. In addition, this SAW layout may be put to use in practical gas sensing applications. The future of SAW gas sensors lies on the development of new IDT structures.

This effort will concentrate on constructing this through lithography methods in order to allow future SAW manufacture, and a vector network analyzer (VNA) will be utilized to compute the scattering parameters. This will be done in order to enable future SAW production.

Acknowledgements. The authors are pleased to acknowledge the Indian Science Technology and Engineering facilities Map (I-STEM) for providing the simulation platform facility and the University of Delhi, funded by the Institution of Eminence (IoE) under the faculty research programme (Ref.No./IoE/2021/12/FRP).

References

1. Kumar, M., Kumar, D., Gupta, A.K.: Fe-doped TiO_2 thin films for CO gas sensing. J. Electron. Mater. **44**(1), 152–157 (2015)
2. Kumar, M., Gupta, A.K., Kumar, D.: Mg-doped TiO_2 thin films deposited by low cost technique for CO gas monitoring. Ceram. Int. **42**(1), 405–410 (2016)
3. Liu, Y., Cai, Y., Zhang, Y., Tovstopyat, A., Liu, S., Sun, C.: Materials, design, and characteristics of bulk acoustic wave resonator: a review. Micromachines **11**(7), 630 (2020)
4. Mandal, D., Banerjee, S.: Surface acoustic wave (SAW) sensors: physics, materials, and applications. Sensors **22**(3), 820 (2022)
5. Barie, N., Rapp, M., Ache, H.J.: UV crosslinked polysiloxanes as new coating materials for SAW devices with high long-term stability. Sens. Actuators, B Chem. **46**(2), 97–103 (1998)
6. Tasaltin, C., Ebeoglu, M.A., Ozturk, Z.Z.: Acoustoelectric effect on the responses of saw sensors coated with electrospun ZnO nanostructured thin film. Sensors **12**(9), 12006–12015 (2012)
7. Ionescu, V.: Design and analysis of a Rayleigh saw resonator for gas detecting applications. Rom. J. Phys. **60**(3–4), 502–511 (2015)
8. Avramov, I., Radeva, E., Lazarov, Y., Grakov, T., Vergov, L.: Sensitivity enhancement in plasma polymer films for surface acoustic wave based sensor applications. Coatings **11**(10), 1193 (2021)
9. Esmeryan, K.D., Avramov, I.D., Radeva, E.I.: Temperature frequency characteristics of hexamethyldisiloxane (HMDSO) polymer coated Rayleigh surface acoustic wave (SAW) resonators for gas-phase sensor applications. Micromachines **3**(2), 413–426 (2012)
10. Parker, T.E., Schulz, M.B.: SiO_2 film overlays for temperature−stable surface acoustic wave devices. Appl. Phys. Lett. **26**(3), 75–77 (1975)
11. Eggins, B.R.: Chemical Sensors and Biosensors, vol. 2. Wiley (2002)
12. Banerjee, S., Leckey, C.A.: Computational Nondestructive Evaluation Handbook: Ultrasound Modeling Techniques. CRC Press, Boca Raton, FL, USA (2020)
13. Shreve, W.R.: U.S. Patent No. 4,081,769. U.S. Patent and Trademark Office, Washington, DC (1978)
14. Ramakrishnan, N., Namdeo, A.K., Nemade, H.B., Palathinkal, R.P.: Simplified model for FEM simulation of SAW delay line sensor. Procedia Eng. **41**, 1022–1027 (2012)
15. Atashbar, M.Z., Bazuin, B.J., Simpeh, M., Krishnamurthy, S.: 3D FE simulation of H_2 SAW gas sensor. Sens. Actuators, B Chem. **111**, 213–218 (2005)
16. Zheng, P., Greve, D.W., & Oppenheim, I.J.: Multiphysics simulation of the effect of sensing and spacer layers on SAW velocity. In: COMSOL Conference 2009, Boston (2009)
17. Jakubik, W.: Theory of saw gas sensor based on bi-layer conductivity changes. Procedia Eng. **47**, 1287–1290 (2012)

18. Nicolas-Debarnot, D., Poncin-Epaillard, F.: Polyaniline as a new sensitive layer for gas sensors. Anal. Chim. Acta **475**(1–2), 1–15 (2003)
19. Fratoddi, I., Venditti, I., Cametti, C., Russo, M.V.: Chemiresistive polyaniline-based gas sensors: a mini review. Sens. Actuators, B Chem. **220**, 534–548 (2015)
20. Sengupta, P.P., Barik, S., Adhikari, B.: Polyaniline as a gas-sensor material. Mater. Manuf. Processes **21**(3), 263–270 (2006)
21. Ho, C.K., Lindgren, E.R., Rawlinson, K.S., McGrath, L.K., Wright, J.L.: Development of a surface acoustic wave sensor for in-situ monitoring of volatile organic compounds. Sensors **3**(7), 236–247 (2003)
22. Stefanescu, A., Muller, A., Konstantinidis, G., Buiculescu, V., Dinescu, A., Stavrinidis, A., Cismaru, A.: SAW GaN/Si based resonators: modeling and experimental validation. In: CAS international semiconductor conference, vol. 1, pp. 193–196. IEEE (2012)
23. Nguyen, V.H., Kaulen, C., Simon, U., Schnakenberg, U.: Single interdigital transducer approach for gravimetrical SAW sensor applications in liquid environments. Sensors **17**(12), 2931 (2017)